CHAPTER IV

RESULTS AND DISCUSSION

4.1 Starch Powder Analysis

Water content, and decomposition temperature (T_d) of the starch powder used in this study were analysed by thermogravimetric analyser (TGA) and the results are shown in Figure 4.1.
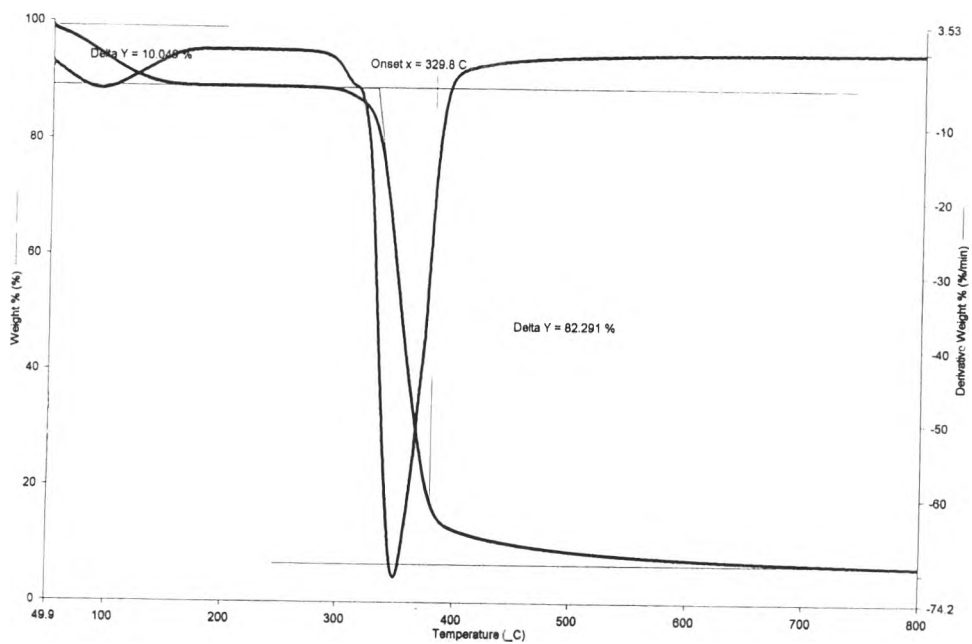

Figure 4.1 TGA thermogram of the starch powder

The TGA thermogram of starch powder shows two steps of weight loss, the first one involves the evaporation of water at about 98°C, which is about 10%. The second peak involves the pyrolytic decomposition of starch and its fraction sets in at the decomposition temperature of 330°C; the decomposition products include carbon dioxide, carbon monoxide, volatile organic compounds, and a carbonaceous residue.

Next, the particle size of the starch powder was measured by Mastrersizer S and the result is shown in Figure 4.2.
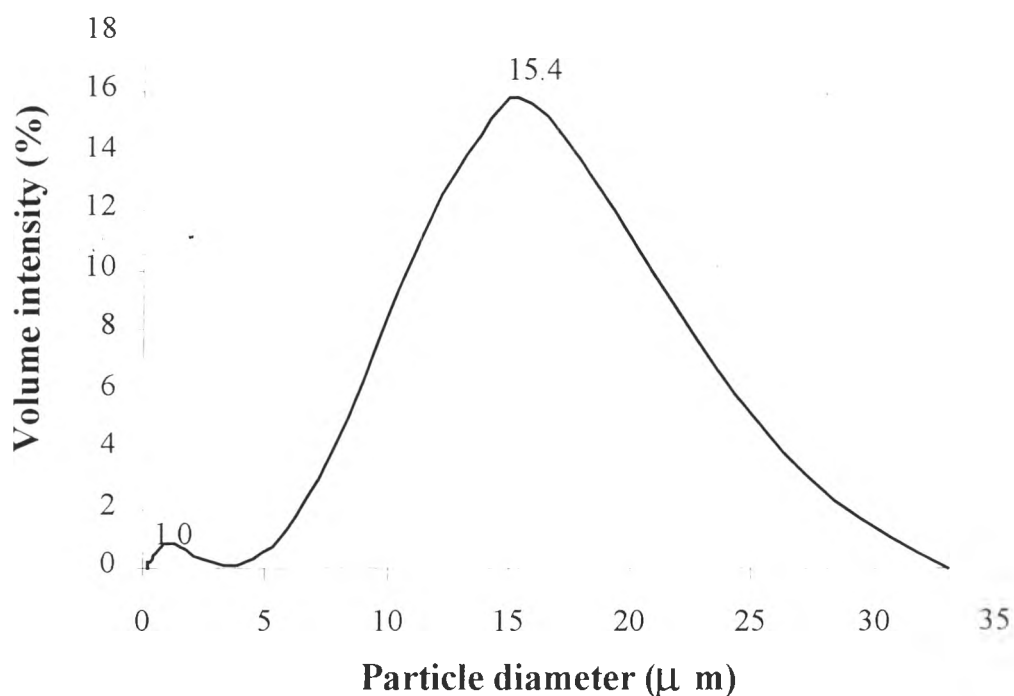

Figure 4.2 Particle size distribution of starch powder in water

It can be seen from Figure 4.2 that the size of starch powder was polydisperse with a wide range of diameter from 0.2 to 33.0 μm and its average particle size diameter was about 15.4 μm. These results agreed well with the typical data reported that the starch is found in nature as crystalline beads of about 15-100 μm in

diameter [7,8]. It also seen the part of the average particle size of about 1.0 μm. This might be due to the fraction of some additives in the starch powder.

4.2 General Characteristics of Natural Rubber Latex

Percentage Total Solid Content (%TSC) and Dry Rubber Content (%DRC) of the high ammonia concentrated NR latex used in this study were determined and the results are shown in Table 4.1.

Table 4.1 Solid contents of NR latex used in this study

Sample number	Total Solid Content (TSC) (%)	Dry Rubber Content (DRC) (%)
1	62.5	60.5
2	62.3	60.7
3	62.4	60.6
Average	62.4 ± 0.1	60.6 ± 0.1

It was found that %TSC was higher than %DRC by about 2%. This might be due to the presence of non-rubber constituents in the NR latex [10].

The particle size distribution of concentrated NR latex measured by using Matersizer S is presented in Figure 4.3.

The curve in Figure 4.3 showed a broad distribution in size of NR latex particles, which varied from 0.33 to 2.5 μm and its average size was about 0.7 μm.

These results agreed well with the typical data reported that the rubber particles in NR latex are naturally polydisperse and average size is about 0.25-0.8 μm [10,11].
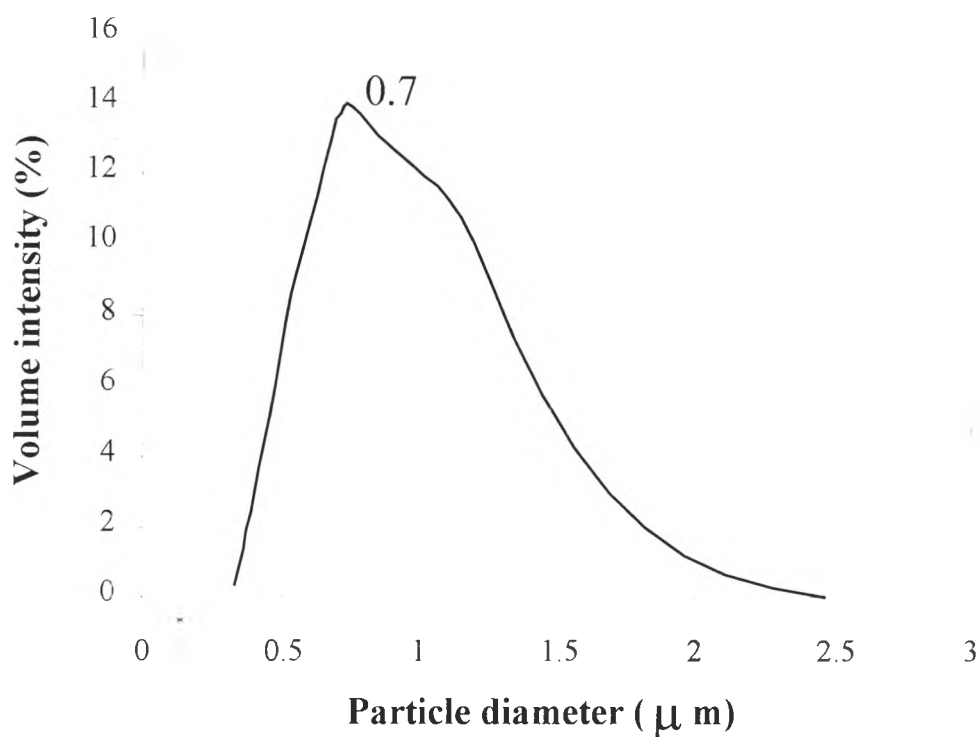

Figure 4.3 Particle size distribution of the concentrated NR latex used in this study

4.3 Foam from Starch and Water

4.3.1 Foaming process of starch and water

The starch composition with a defined amount of water according to Table 3.1 was heated to approximately 70 °C. At this temperature the granules starch began to swell and the starch becomes hydrated within 10-15 min, then a substance of high viscosity was formed. This can be said that the starch exhibits a gelatinization

phenomenon. The gelatinization could not obtained, when the amount of water lower than 100% by weight of the starch and the temperature under 60 °C. Nevertheless, this gelatinization was not completely formed in this step. It could be seen in Figure 4.4 that the mentioned gelatinized starch, which was observed under the plane of a polarized light microscope, exhibited the birefringence phenomenon. Although the starch was not completely gelatinized, this partially destructurized starch is sufficient to form the foam by compression molding. We could thus assume that the gelatinization would be further completed in the subsequent foaming process. This can be proved by viewing the thin film, which was cut from the foams obtained, under the plane of a polarized light microscope. The results have been shown that the thin film does not exhibit the birefringence. The results agreed well with those reported by Colonna et al. [7]. They reported that all starches exhibit a pure gelatinization phenomenon, which is the disorganization of the semi-crystalline structure of the starch granules during heating in the presence of a water fractor > 0.9. They also found that the gelatinization occurred in two stages. The first step was found at around $60 - 70°C$, corresponding mainly to the swelling of the granules with a limited leaching. The second step found at above $90°C$ implied the complete disappearance of granular integrity by an excessive swelling and solubilization.

The foaming process of starch can be described as follows. The viscous substance was introduced into the hot mold, and was subject to the temperature range of 130 to 180°C, and the pressure at $50 - 110$ $kg_f cm^{-2}$. The pressure caused the water to become superheated and the resulting pressure drop turned the water into steam and a foaming process takes place. The foams solidified as they were cool and passed through their T_g.

These results indicated that the starch foam formed as the starch gelatinizes, expands, and dries in the compression mold. This is similar to the foaming process of starch by the extruder cited in literatures elsewhere [1-5].

From the experiments it was also found that if the highly, but not yet completely gelatinized starch, which is easily observed by a naked eye as the transparently viscous substance, was used instead of the partially gelatinized starch. The former does not expand or foam during the compression process. Our observation is in agreement with Shogren's work [3], which claimed that the starch dispersions in which the granules have been completely disrupted (by jet-cooking, for example) do not foam during baking. On the contrary, if the starch in the swelling stage was subjected to the hot mold, it cannot produce the foam. These results indicated that the partly gelatinized starch is needed to produce the foam by this foaming process. However, the relation between the appropriate degree of gelatinization of the starch and the foaming properties needs further investigation.

A temperature, in which the foaming process can be performed, was in the range of from 130 to 180°C. If the temperature is lower than 130°C, the foaming does not occur, because the temperature is not sufficient to make the gelatinized water become superheated and there are not sufficient steam to generate the foam. On the other hand, when the temperature exceeds 180°C, the starch is deteriorated.

In this foaming process, it was also observed that water acts as a mold release agent to prevent sticking of the starch to the mold, besides its main function as a blowing agent.
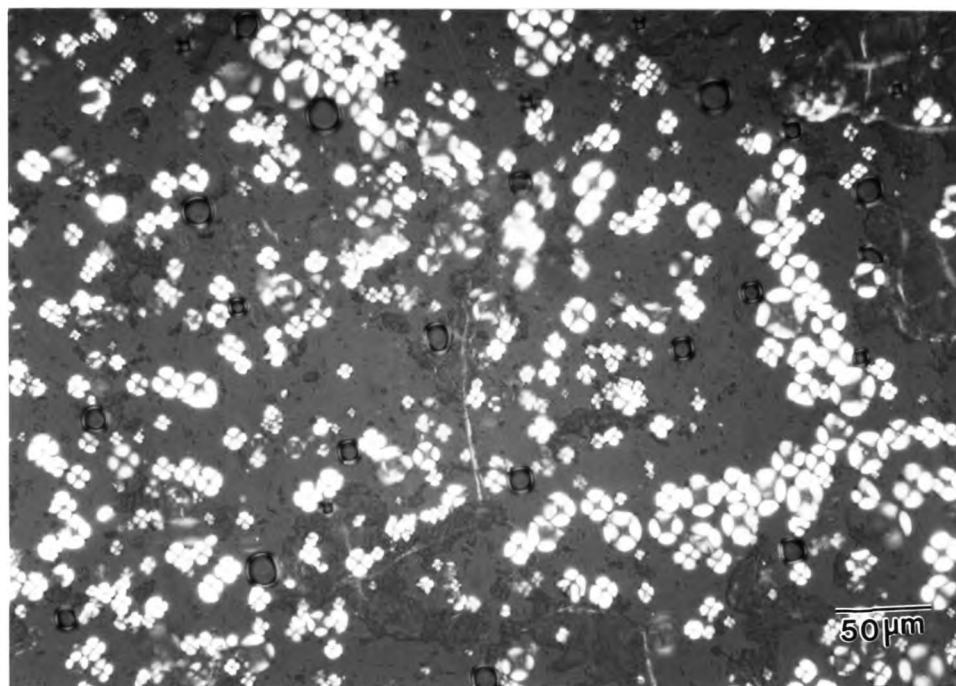
Figure 4.4 Photograph of the gelatinized starch observed with a plane

polarized light (at 20x magnification).

4.3.2 Cell structure of foam from starch and water

Since water acts as a "blowing agent" in the system of expanded-foam from starch and water, the effect of water content on the foaming process and the cell structure of the foam were studied by preparing a product using the formula in Table 3.1. The suitable amount of water will be choose and use in the next experiment, which reveal the incorporate NR latex into the starch to produce a foam.

The resulting products were collected and evaluated for different characteristics as shown in Table 4.2 and Figures 4.6-4.7 All products gave a uniformly closed cell structure, except for those having 250 and 300 % water content were non-uniform cell structure. A closed cell structure is defined as the one having largely nonconnecting cells and the cells are fully separated by matrix material, as apposed to open cells which are largely interconnecting or defined as two or more cells interconnected by a broken, punctured or missing cell wall [2]. The schematic of the closed and open cell structure is illustrated in Figure 4.5.
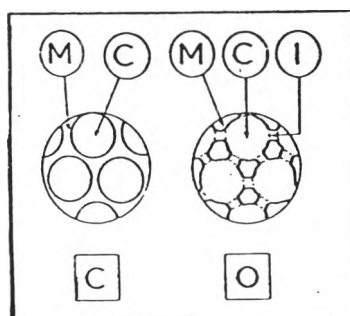

Figure 4.5 Morphology of the foam showed closed and open cell structure

[C] Closed cell; [O] Open cell;

(M) Matrix; (C) Cell; (I) Interconnection

It could be explained that when water content exceeded 200% by weight of the starch, a resulting high steam level in the foaming process caused an insufficient stability of the cell wall and a non-uniform cell size of the foam was thus produced. The open cell structure is found abundantly in this foam. On the contrary, when water content was lower than 150% by weight of the starch, a resulting lower steam level

caused a poor condition of foaming as a difficulty to flow in the mold, thus foamed and un-foamed parts coexisted. The results of foaming are shown in Figure 4.6.

Figure 4.6 shows the condition of starch foaming when more water was added to the starch. During the foaming process of the gelatinized starch and water, the water in the starch tended to pop up when the mixture was heated. In Figure 4.6a, when the water content in the gelatinized starch was low, the starch foam was not in a good appearance and shape, because all water was absorbed by the starch molecules. There was not enough free water to form water droplets in the foam to form a closed cell. When more water was added, the foaming process was improved because the excess, free water surrounding the starch molecule could form many droplets in the foaming process as shown in Figures 4.6b and c. However, when an extremely excess amount of water was added, the water droplets around the starch molecules, as shown in Figures 4.6d and e, became too large to withstand the foaming stress, leading to the instability of the foam structure.

The cell structure of the foam produced was viewed under an optical microscope, and the photographs are shown in Figure 4.7.

As mentioned previously, the cell structure of the foams obtained were all closed cells. From Figure 4.7, the photographs at 20x magnification were clearly shown the closed cell structure of the foam. The cell sizes of all foams were polydisperse and the cell sizes tended to increase with increasing the water content in the composition.

Table 4.2 The compositions and the characteristics of the foams

Sample	Water content (% by weight of the starch)	Appearance of foaming	Cell structure
S/W-1	100	Poor	Closed
S/W-2	150	Very Good	Closed
S/W-3	200	Very Good	Closed
S/W-4	250	Fairy Good	Non-uniform
S/W-5	300	Fairy Good	Non-uniform

In order to obtain the proper starch foam structure by this system, the total water content of the starch composition should be from about 150 to 200 % weight based on weight of the dry starch in the composition.
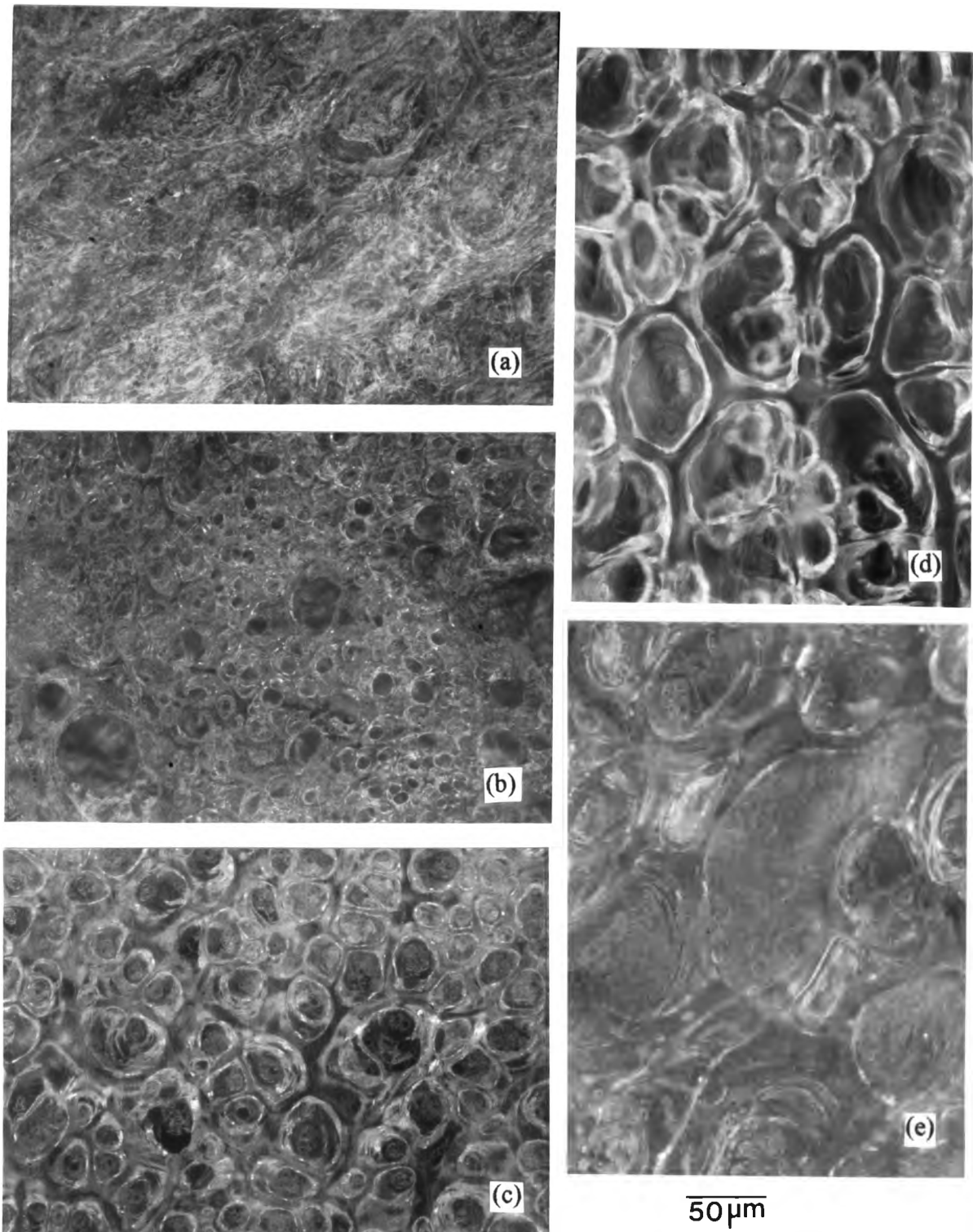
Figure 4.6 Optical micrograph (20x magnification) of appearance of the

starch foam with increasing the water content (a): 100%; (b):

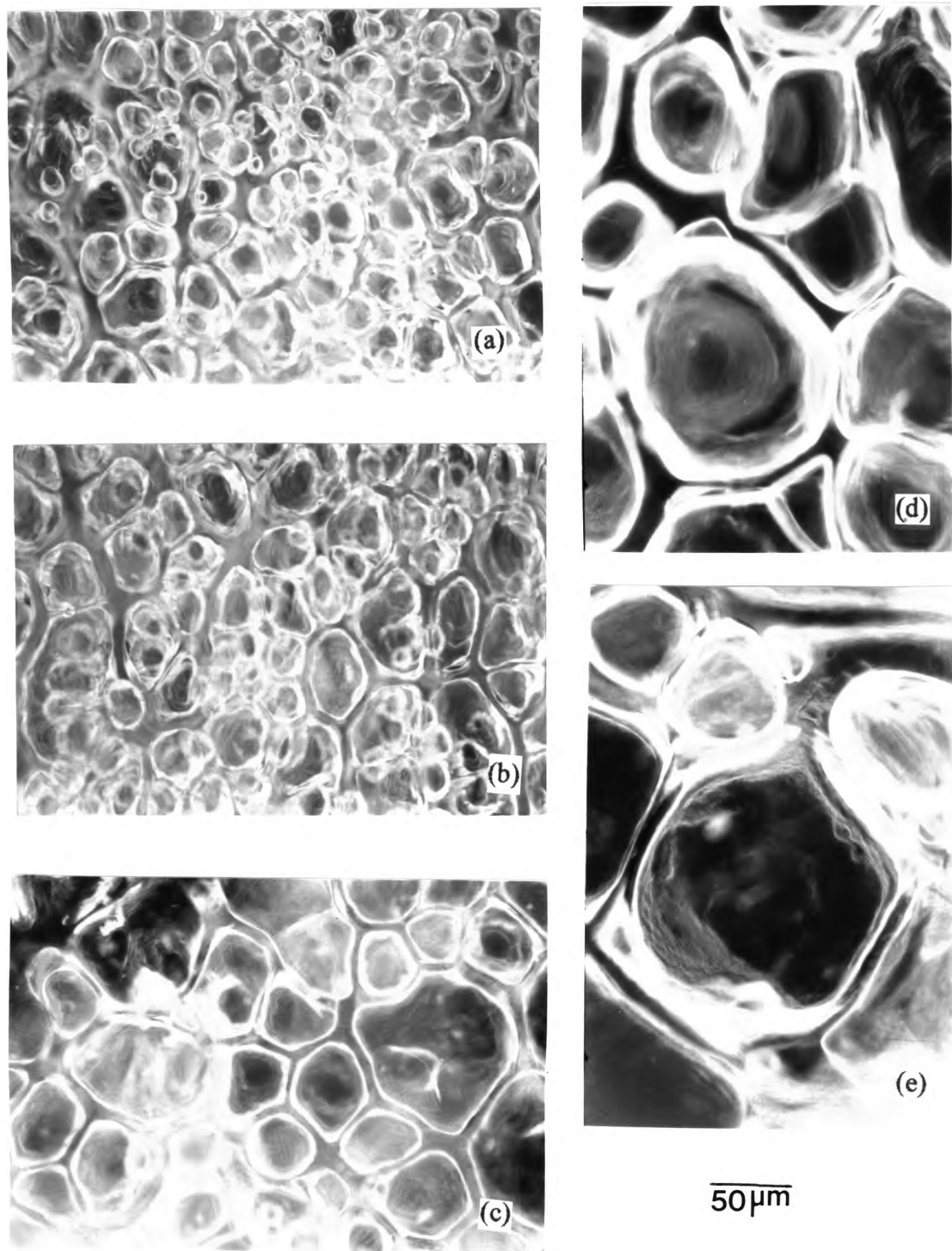150%; (c): 200%; (d): 250%; (e): 300%

Figure 4.7 Optical micrograph (20 magnification) of the cell structure of the foam from starch and water in various water contents: (a): 100%; (b): 150%; (c): 200%; (d): 250%; (e): 300%.

4.4 Stability of the NR latex dispersed in the gelatinized starch

The blending of the starch and NR in this study were performed by mechanically molten blending at the temperature of 70°C. At this temperature, the destabilization of NR in the starch will occur and the NR portion cannot be directly dispersed in the gelatinized starch.

A non-ionic surfactant (Nonidet P40) was selected to stabilize the NR latex in the gelatinized starch. The polyethylene glycol part of Nonidet P40 protruding in the water boundary would provide steric stabilisation to the suspended NR particles.

Before preparing starch/natural rubber (S/NR) blends at various ratios, the suitable amount of the surfactant required to keep stabilized well, dispersed NR in the gelatinized starch and provides a good NR dispersion was explored. The non-ionic surfactant at various amounts was firstly added to the NR latex and stirred at room temperature for a few seconds to obtain a stabilized NR latex. The stabilized NR latex then was blended with the gelatinized starch. The appearance of the blend was visually noticed as indicated in Table 4.3.

It was observed that the low amounts of Nonidet P40, e.g., 0.5 and 1% by weight of NR caused coagulation of the NR particles. Thus, the mixture obtained shown the heterogeneous appearance. An attempt was made to illustrate these in Figure 4.8. In these cases, the amount of Nonidet P40 on the surface of NR latex might not be enough for keeping the NR stable and the NR particles tended to agglomerate. On the contrary, the coagulation of NR particles could not be observed when using high amounts of Nonidet P40, e.g., 1.5, 2.0 and 2.5 % by weight of NR. It could be explained that the sufficient amount of Nonidet P40 on the surface of NR

particles, e.g., 1.5% by weight of NR or above, enhanced its stability by steric stabilisation. It should be emphasized that the minimum amount of Nonidet P40 used to prevent the coagulation of NR latex and to disperse NR latex on gelatinized starch was 1.5% by weight of the NR latex.

Table 4.3 Effect of the amount of Nonidet P40 used for dipersing the NR latex in the gelatinized starch.

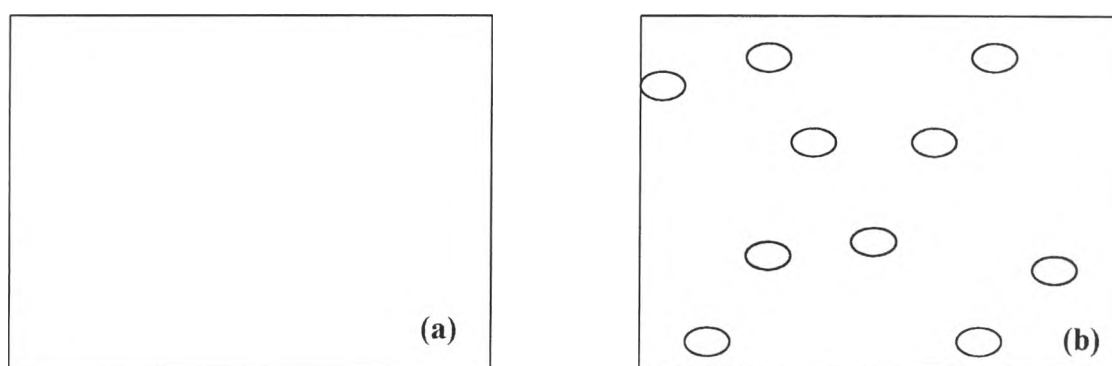| Sample	Nonidet P40 (% by weight of NR)	The appearance of Starch/NR latex blend
S/S-1	0.5	Heterogeneous
S/S-2	1.0	Heterogeneous
S/S-3	1.5	Homogenous
S/S-4	2.0	Homogenous
S/S-5	2.5	Homogenous

Figure 4.8 A proposed model of starch and NR blend: (a) homogeneous blend, and (b): heterogenous blend, ⬭ represents the agglomerated NR particles

4.5 Effect of the NR content on the blending and foaming processes

For the mechanically melt blend of starch/NR in the presence of non-ionic surfactant, we can observe the behavior of the blend as follows. The time used for the gelatinization of the mixtures was increased with increasing the NR content. One explanation might be that the NR particles probably act as a mechanical resistance, thereby slowing the granule swelling somewhat during the melt blending process. When the NR content exceeds 50%, it inhibits the gelatinazation. Thus, the resulting mixture obtained cannot form a foam in the compression molding process. This phenomenon is similar to the un-foamed starch in a swelling stage, as mentioned earlier. From an experimental point of view, it was necessary that the maximum loading of NR filled in the blending regarding their processing properties was found to be 50%.

4.6 Phase Morphology of the blend

The blends of starch and NR were examined initially by the polarized light microscopy. Small amounts of samples were taken from the bulk of the blends and spread on the glass slide. Paraffin oils were then poured onto the sample to enhance the phase contrast of the two phases in the blends. The phase morphologies of the gelatinized starch alone and gelatinized starch/NR blend were shown in Figure 4.10. For a comparison, a photograph of starch granules from the starch powder is included in Figure 4.9.

As previously mentioned in Section 4.3.1 that the gelatinization of starch was not completed in the first heating step, but it would continue to be complete in the subsequent foaming process. As such the crystalline structure of starch granules still exhibit. We can still observe the starch granules from the said gelatinized starch.

Contrary to the one phase of gelatinized starch, the photograph of the blends show another phase, which is believed to be the phase of NR. For the sizes of the two phases in this system, it is very difficult to measure because the measurement technique is not yet established. The spreading of the sample onto the glass slide manually might cause particle size distortion from its original blending state.
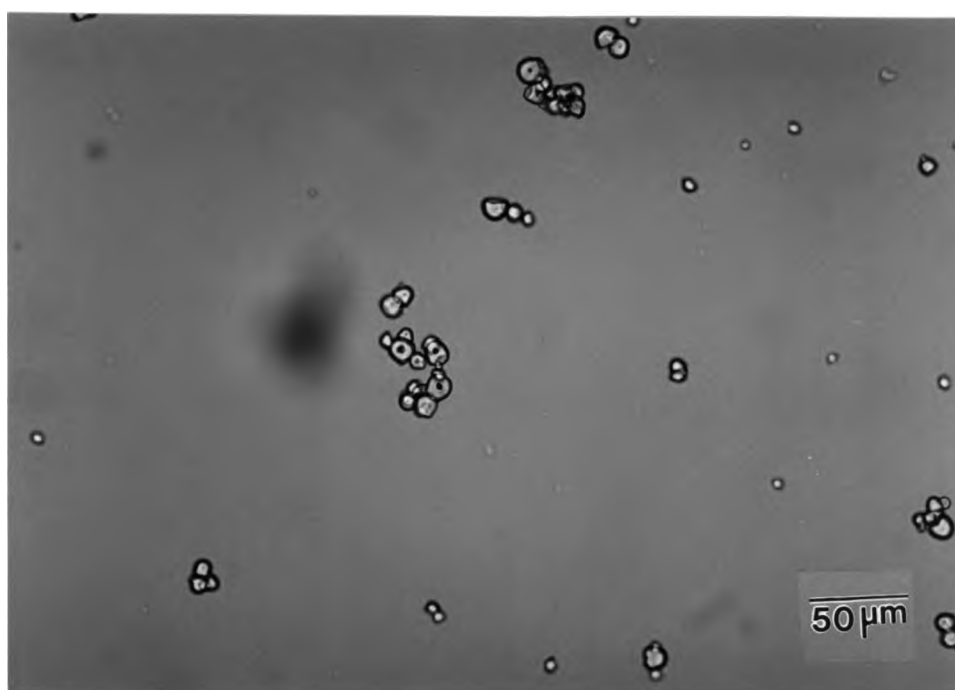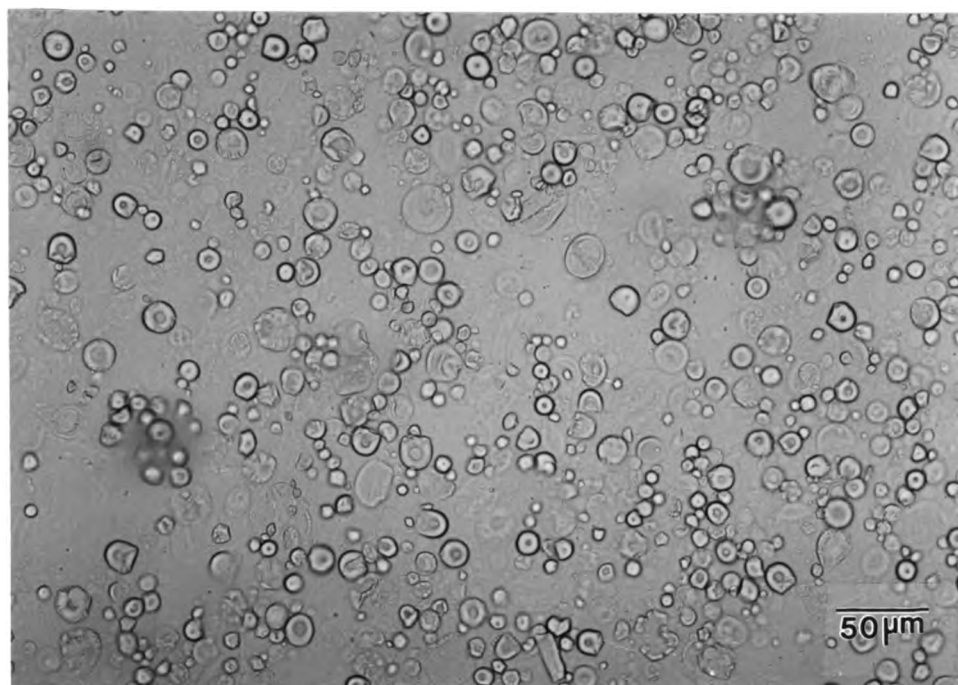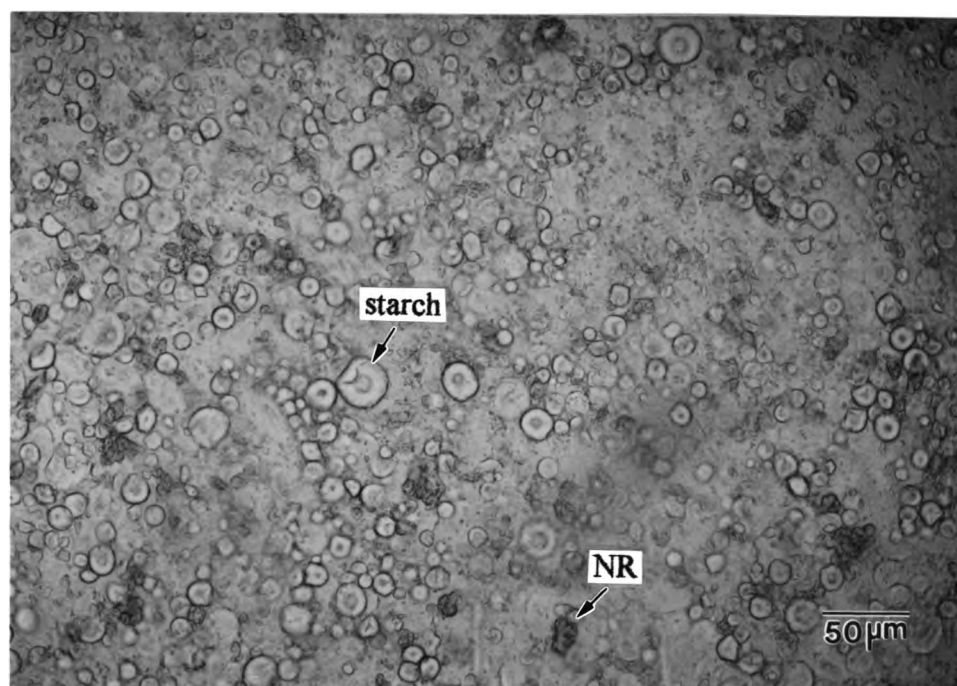

Figure 4.9 Photograph of starch granules from the starch powder observed under a plane polarized light at a 20x magnification

(a)

(b)

Figure 4.10 Optical photographs of (a) gelatinized starch, and (b) gelatinized

starch/NR blend observed under a plane of the polarized light microscope

at 20x magnification.

4.7 Morphology of the Foams

Scanning electron micrographs of the starch foam are shown in Figures 4.11-4.12. Cross-sectional views [Figure 4.11] show that all foams have dense outer skins with small cells and less dense interiors with large cells. Being close to the hot mold at the foaming stage the outer skin is more dense because the starch paste dries rapidly and therefore cannot expand very extensively. The interior of the foam contains mostly large cells due to the large amounts of steam venting outside the mold and a consequent cell rupture.

When considering the cell wall thickness of the foams, it shows clearly in Figure 4.12 that the starch/NR foams have the thicker cell wall than that of the foam from the starch alone. The thicker cell wall contributed to the higher mechanical properties as seen from the higher compressive strength of the starch/NR foams over the starch foam. However, at the present study, the detailed information on the exact location of NR particles in the foamed starch/NR blends obtained is not readily available. From the information of the phase morphology of the blend in Section 4.5, it can be assumed that the NR particles can dispersed quite well in the starch as a strong structure contributor. When it is used, a foam is formed and the NR is served to increase the cell wall thickness and the strength of the foams.
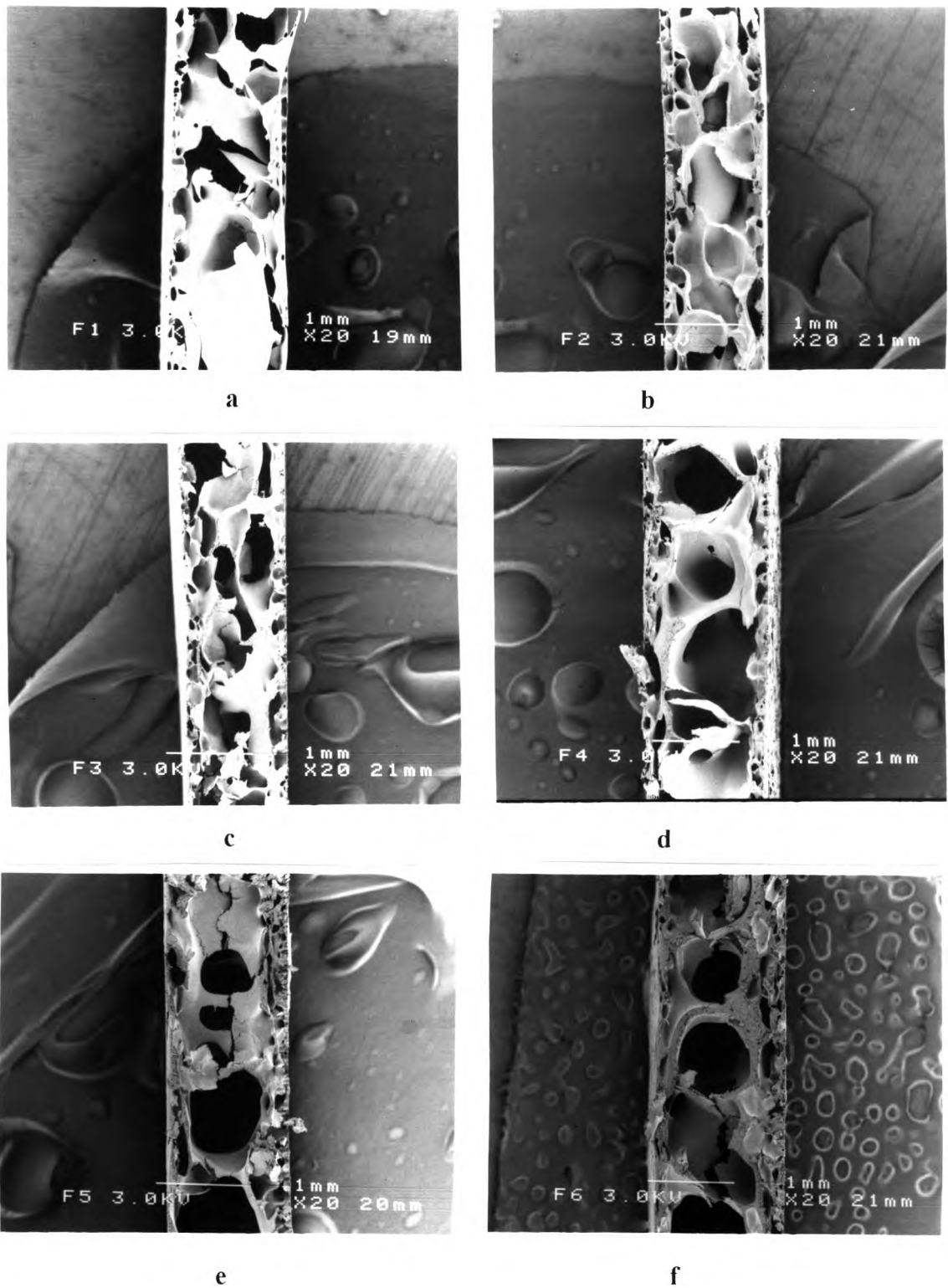
Figure 4.11 Scanning electron micrograph of cross sections of starch foams at

20x magnification: (a) starch; (b) NR 10%; (c) NR 20%; (d) NR 30%
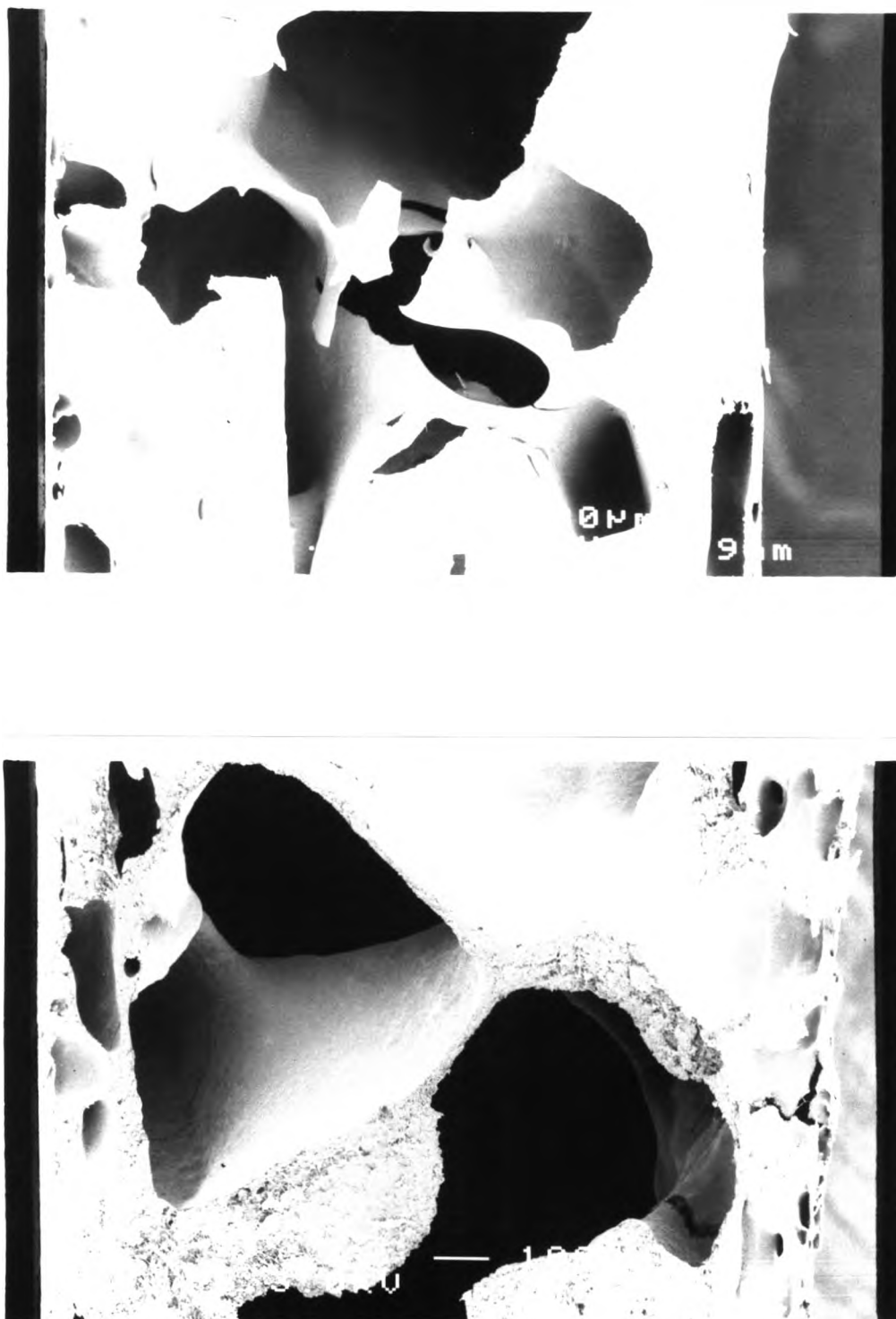
(e) NR 40% (f) NR 50%

Figure 4.12 Scanning electron micrographs of cross sections of (a) starch and,

(b) NR 30% foams at 75x magnification.

4.8 Compressive Strength of the Foams

The aim of the present study is to prepare the foam from starch/NR blend to be used as a shock absorbing material. Such a foam should give appropriate compressive strength properties because it is used in a package when compression usually takes place during a package transportation.

The compressive strength is usually reported at some definite deflection (5% or 10%) [16]. Compressive strength tested in this study is the maximum force required to compress the foam at 50% strain. High compressive strength implies that the foams resist a compression. The effects of NR level and the added of benzoyl peroxide to the blends on the compressive strength of starch and starch/NR foams are given in Figures 4.13-4.14 and Table 4.4.

Based on the data, it is clearly shown that increases in the NR contents increase the compressive strength of the foams in the range of 20-118% as showed in Table 4.5. Similarly, the starch/NR foams with 30% of NR and various concentrations of benzoyl peroxide shows the trend increasing in the compressive strength with increasing benzoyl peroxide content in the range of 42-233% as showed in Table 4.6. These results are in a good agreement with the morphology of the foam shown in Section 4.7. This result confirms that the thicker the cell wall, the higher the compressive strength. In other word, the thicker cell wall contributes the stronger compressive strength of the foam.

Considering the characteristics of the two polymers, it can be explained that NR are more elastic. When it is blended with a brittle starch, it would tend to reduce the brittle failure of the blend.

As expected, the significantly higher compressive strength of the foams cured with benzoyl peroxide was observed. It is probably due to the crosslinks of the NR molecules in the foams. Consequently, the foam strength is increased. The gradual increase the compressive strength with the lower amounts, e.g., 2 to 3% of benzoyl peroxide, was observed. On the other hand, the compressive strength is greatly increased when the higher amounts, e.g., 4 to 5% of benzoyl peroxide, was used. The results indicated that the low concentration of benzoyl peroxide might be insufficient to promote the high degree of crosslinking reaction in the NR under the mild condition used to process the foams.
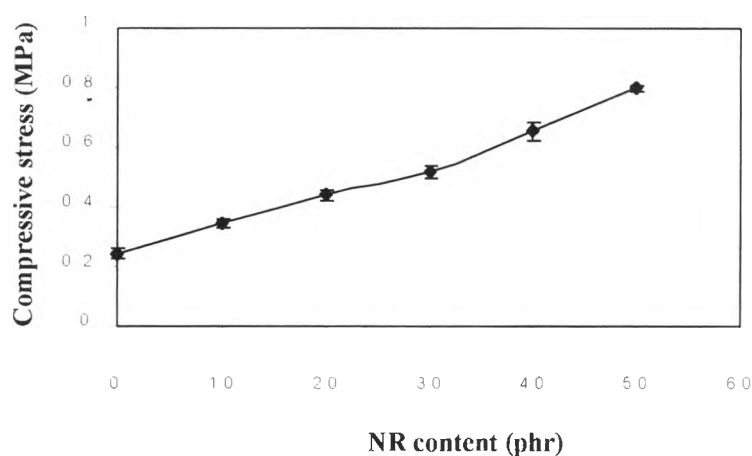

Figure 4.13 Compressive strength of the starch/NR foams without benzoyl Peroxide.
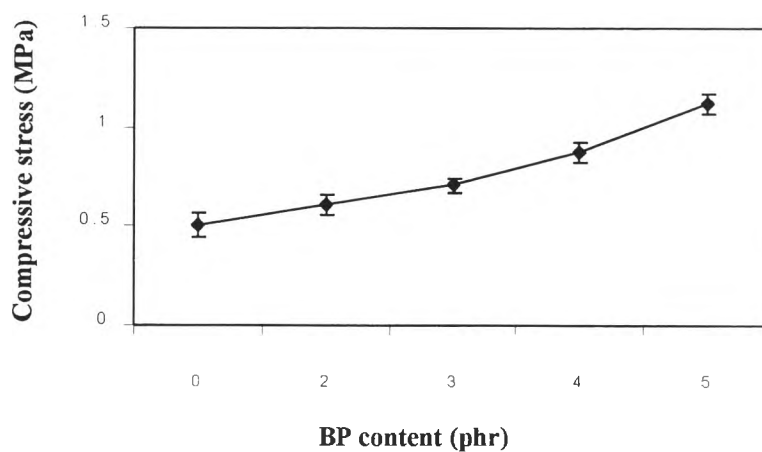
Figure 4.14 Compressive strength of the starch/NR foams with

benzoyl peroxide.

Table 4.4 Compressive strength of the foams

Sample Code	Compressive strength at 50% strain (MPa)					Data	X	SD
	1st	2nd	3rd	4th	5th			
S/NR-1	0.24	0.22	0.26	0.24	0.26	5	0.24	0.017
S/NR-2	0.34	0.34	0.35	0.36	0.33	5	0.34	0.012
S/NR-3	0.44	0.42	0.44	0.46	0.44	5	0.44	0.014
S/NR-4	0.49	0.53	0.54	0.52	0.50	5	0.52	0.020
S/NR-5	0.65	0.62	0.64	0.70	0.66	5	0.65	0.031
S/NR-6	0.80	0.81	0.78	0.79	0.80	5	0.80	0.012
BP 0%	0.53	0.55	0.56	0.50	0.40	5	0.51	0.065
BP 2%	0.59	0.55	0.68	0.64	0.60	5	0.61	0.052
BP 3%	0.69	0.72	0.66	0.71	0.76	5	0.71	0.037
BP4%	0.86	0.91	0.94	0.82	0.85	5	0.88	0.050
BP5%	1.18	1.17	1.10	1.05	1.07	5	1.11	0.056

Table 4.5 The percentage increase in compressive strength of the foams with varies
NR content

NR latex content (%)	Increasing in compressive strength (%) compare with the starch foam
10	42
20	83
30	117
40	171
50	233

Table 4.6 The percentage increase in compressive strength of the foams with varies
benzoyl peroxide content

Benzoyl peroxide content (%)	Increasing in compressive strength (%) compare with 0% benzoyl peroxide content
2	20
3	39
4	73
5	118

4.9 Dynamic mechanical properties of Starch/NR Foams

Many polymers show characteristic modulus changes and absorption peaks at specific temperatures, which are used as a means of "fingerprint" polymer types and for identifying important properties, such as the α relaxation. On the other hand, it is often possible to relate peaks in E″ and tan δ to a particular type of molecular motion in the polymer. In general, the peaks can be regarded as due to a damping effect, and occur at characteristic frequencies of some molecular motion of the polymer structure. The fact that dynamic mechanical testing can be used to follow the main chain and side-group motion in polymers, making it a powerful technique for the characterization of polymer structures and in particular of complex porous materials. An important feature to be characterized in foamed samples, for future applications, is the particularly strong damping, which occurs at the α relaxation temperature [26]. The advantage of using the tan δ curve is that its behavior is independent of the sample geometry, and that the observation of the peaks is easier than with the E″ curve [26,27].

In all the experiments, the tan δ trends with the temperature were followed. Each peak in the tan δ curve was characterized by the magnitude of the maximum (tan δ_{max}). The temperature at the maximum tan δ is defined as T_g of the specimen. The foams mentioned in Tables 3.3 and 3.4 were subjected to the DMA measurement to observe the dynamic mechanical properties. The results are shown in Table 4.7 and Figures 4.15-4.19.

4.9.1 Effect of NR

For the DMA thermograms of the starch/NR foams without benzoyl peroxide, it could be explained as follows. The storage modulus (E'), which reflects the elastic behavior of the material, showed a great difference between starch and starch/NR foams in the whole range of measuring temperature as indicated in Table 4.5 and Figure 4.15. These results indicated that, when adding NR component to the blend, the elastic properties of the foams are increased. This is the contribution from the characteristics of NR, which have the much higher elasticity.

The effect of NR loading on the mechanical properties of the foam was further investigated by considering the value of tan δ. As mentioned earlier, the maximum in tan δ is used as T_g. From Table 4.5 and Figure 4.15, T_g's of the starch/NR foams were found to be approximately constant in a range of –53 to –54°C. This T_g value is corresponded to the temperature of the NR component as could be seen from Figure 4.19. In case of the foams, the magnitude of tan δ is shown proportionally to the NR content.

In theory, mechanical method is one technique used to assess the molecular response of a polymer in blends with other polymers. In a highly phase-separated polymer blend, the transitional behavior of the individual components will be unchanged. Likewise, in a miscible blend, a single and unique transition corresponding to the glass transition will appear [28]. Therefore, in the case of our study, it could be confirmed by this technique that the blend of the two polymers of starch and NR is the incompatible blend.

In addition, attention should be focused on the tan δ of starch foam. It could be seen that the temperature at which the maximum tan δ occurred was about 23°C. This is the glass transition temperature of starch. For the starch/NR foams, it was observed that the tan δ at this region disappeared. It is anticipated that the dynamic mechanical properties of the foams was governed mostly by the NR counterpart. However, this explanation needs more experimental work on information on the phase morphology of the foams.

4.9.2 Effect of Benzoyl Peroxide

The effect of crosslink density of NR, which was varied by changing the quantity of benzoyl peroxide from 2-5 phr is shown in Table 4.7 and Figures 4.17-4.18. It can be seen that increase in the peroxide content increased the storage modulus. The tan δ_{max}, on the other hand, decreased with the increase of benzoyl peroxide as shown earlier. When the crosslink density of the blend was increased, the molecular motions become more restricted, causing the storage modulus to increase, and the loss energy due to the molecular motions (tan δ) to decrease. Considering the temperature at which the maximum tan δ peak occurred, the shift of T_g value to the higher value, from approximately –53 to –50°C was observed. This also corresponded to the restriction of the molecule motions when crosslinking reaction took place.

Based on DMA results, it could be concluded that the storage modulus of the foams increased with increasing NR content, because the NR component has more elasticity, which helps promote the elasticity to the whole foam. The significant increase in the storage modulus was found when 2-5% of benzoyl peroxide by weight

of NR was added to the blends. Crosslinking reaction of the NR contributed to further increase in storage modulus.

Table 4.7 The storage moduli (E′), loss moduli (E″), T_g, and tan δ of the starch/NR Foams

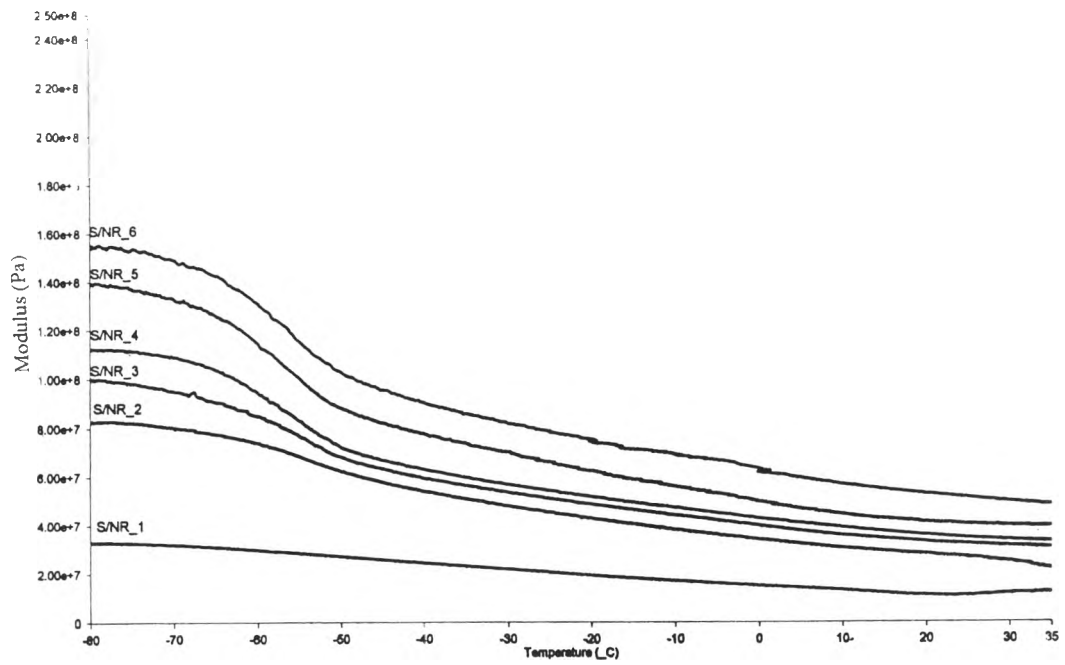| Sample	E′ x 10⁻⁸ At –80°C (Pa)	E″ x 10⁻⁶ at -80°C (Pa)	T_g (°C) Starch	NR	Tan δ Starch	NR
S/NR-1	0.32	0.31	22.9	-	0.21	-
S/NR-2	0.83	0.81	-	-53.9	-	0.12
S/NR-3	1.00	0.81	-	-53.7	-	0.13
S/NR-4	1.12	0.94	-	-54.7	-	0.14
S/NR-5	1.40	0.87	-	-53.7	-	0.17
S/NR-6	1.55	0.99	-	-53.6	-	0.19
BP 0%	0.95	0.65	-	-53.1	-	0.15
BP 2%	1.11	0.90	-	-53.0	-	0.16
BP 3%	1.39	1.01	-	-50.9	-	0.14
BP 4%	1.47	1.07	-	-50.5	-	0.11
BP 5%	2.23	1.33	-	-51.9	-	0.10

Figure 4.15 The storage moduli of the starch and starch/NR foams

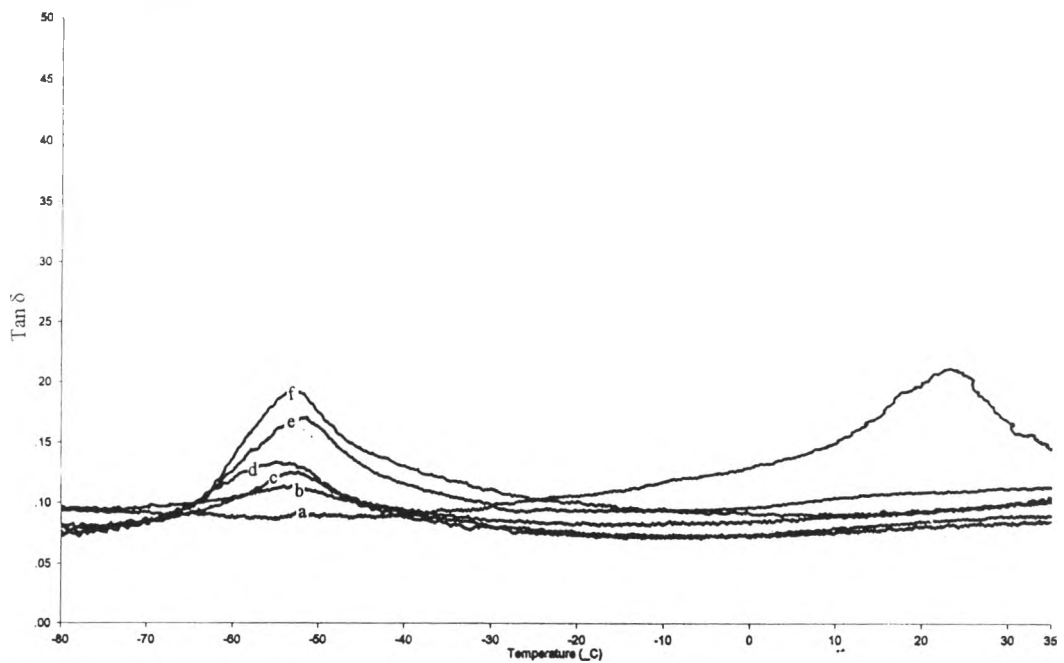**Figure 4.16** Tan δ and T_g of the starch and starch/NR foams with various NR

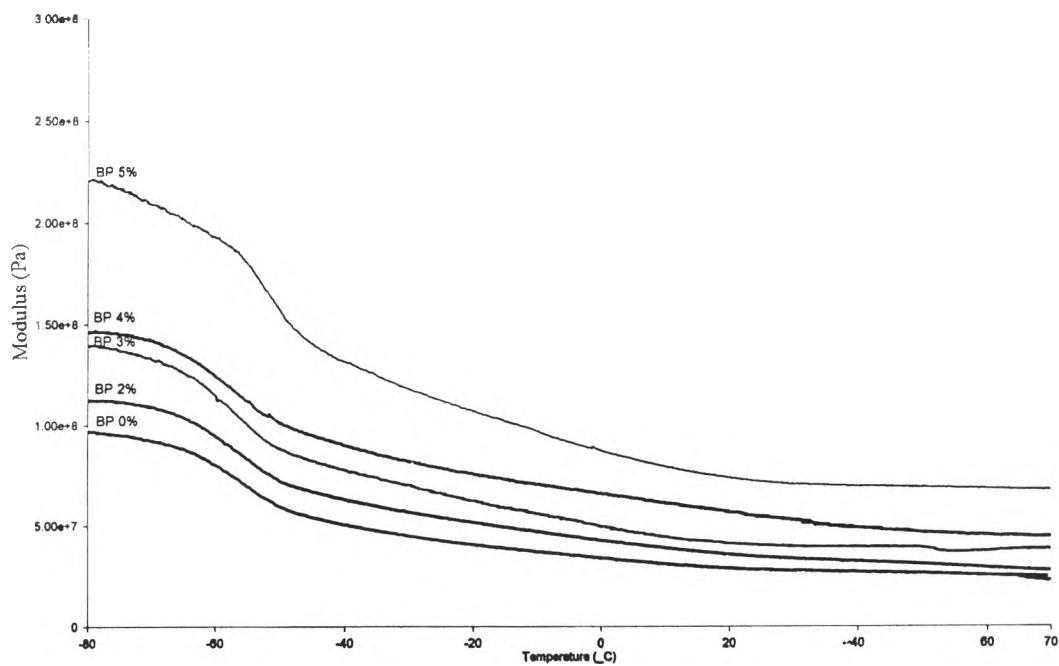content: (a) starch ; (b) NR 10% ; (c) NR 20% ; (d) NR 30% ;

(e) NR 40% , (f) NR 50%

Figure 4.17 The storage moduli of the starch/NR foams with various
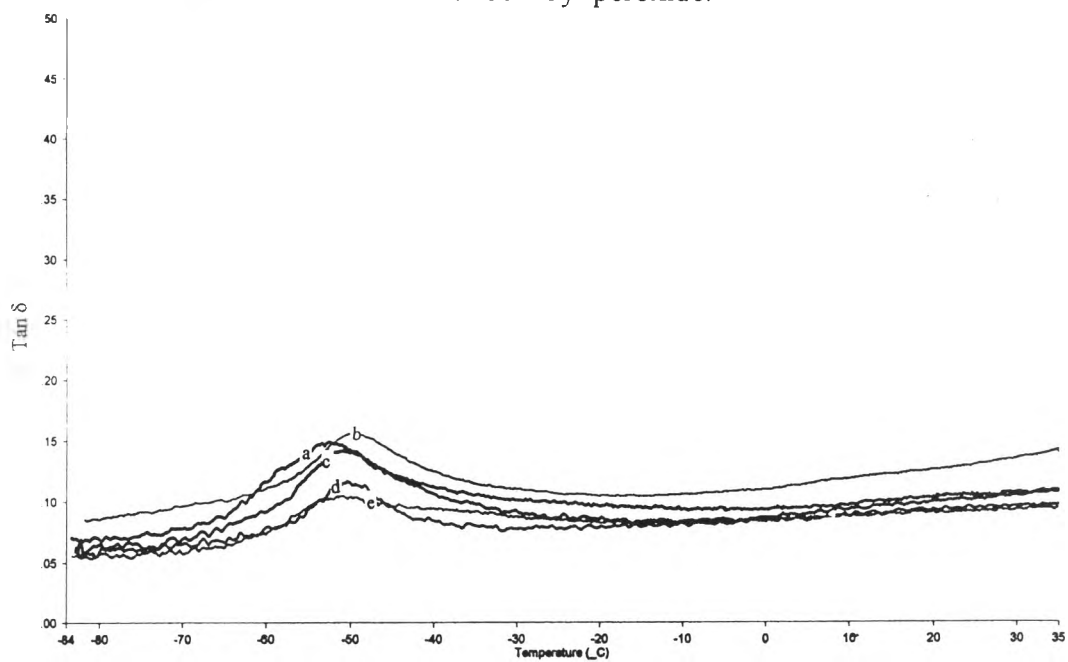
concentrations of benzoyl peroxide.

Figure 4.18 Tan δ and T_g of the starch/NR foams which adding various

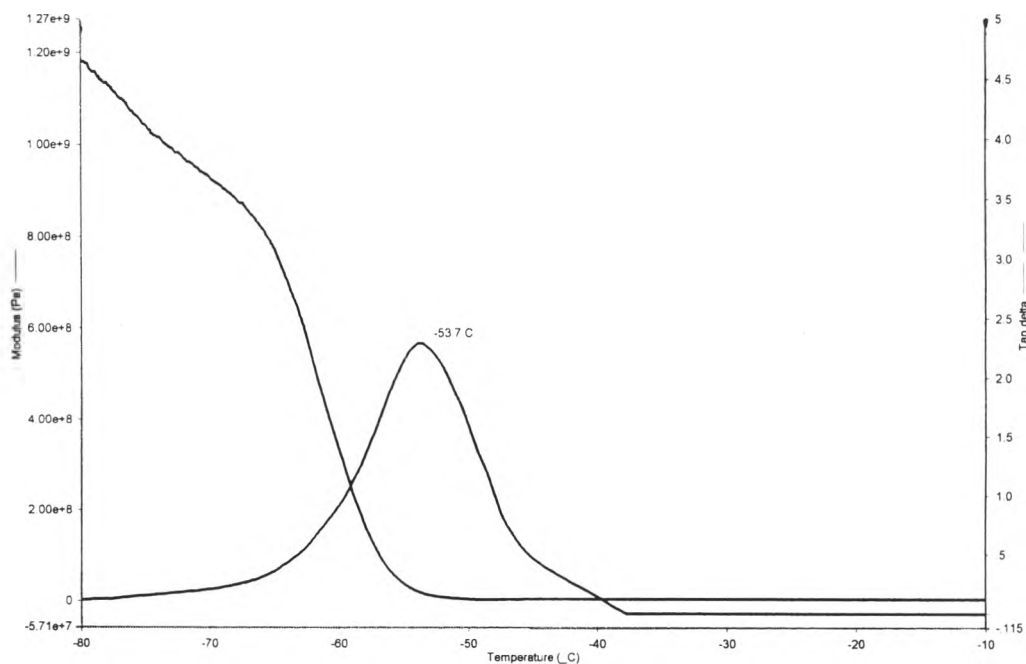concentration of benzoyl peroxide: (a) 0% (b) 2% (c) 3% (d) 4%

(e) 5%

Figure 4.19 Storage modulus, Tan δ and T_g of the NR latex

4.10 Effect of Calciun carbornate

To study the effect of calcium carbonate addition to the blend of starch and NR, 5-30% of calcium carbonate by weight of the dry starch was added to the blend in the mixing step. Calcium carbonate use in this study is the grade without any threatment on the surface. The average particle size diameter as measured by Master sizer is 4.75 μm.

The resulting foams were then tested for the compressive strength and dynamic mechanical properties. Morphology of the foam was examined by SEM. The results are shown in Tables 4.8-4.9 and Figures 4.19-4.20. It is clearly seen that when the content of calcium carbonate is 5% the properties of the foams did not differ from that without calcium carbonate. When the contents of calcium carbonate are increased (15-

30%), the compressive strength of the foams increased by 69-148% as showed in Table 4.10. The storage modulus of the foams are also increased. However, when the calcium carbonate content is 30% we can observe by a naked eye that the particles of calcium carbonate stay on the surface of the foam, i.e. blooming of calcium carbonate takes place. The foams containing calcium carbonate have more hardness and brittleness than that without calcium carbonate. The same result was also observed by Kakinoki et al [4]. They reported that when 0.5-3 % of calcium carbonate by weight of the starch were added to the starch in the manufacture of the foam-expanded material, although the degree of expansion of the material decreased and its specific gravity increased by 5% or more, there was no difference as regards to the strength and resilience of the calcium carbanate filled starch/NR foam.

It could be concluded that calcium carbonate can be added to the starch/NR blend in the range of 5-30%. The compressive strength and the storage modulus of the foams increased with increasing content of calcium carbonate when its content was higher than 5%. Likewise, the hardness and brittleness of the foams of the foams also increased.

One important phenomenon worths mentioning about the addition of calcium carbonate. The blend added with calcium carbonate was easily removed from the blending container and compression mold. One plausible explaination is that calcium carbonate might act as a spacer in which it resides at the surfaces of the blend, apart from acting as a filler of the blend.

Table 4.8: Compressive strength of the foam with and without calcium carbonate

Sample Code	Compressive strength at 50% strain (MPa)					Data	X	SD
	1st	2nd	3rd	4th	5th			
$CaCO_3$ 0%	0.54	0.53	0.50	0.52	0.50	5	0.52	0.017
$CaCO_3$ 5%	0.51	0.54	0.52	0.55	0.51	5	0.54	0.018
$CaCO_3$ 15%	0.88	0.92	0.87	0.82	0.90	5	0.88	0.038
$CaCO_3$ 30%	1.31	1.24	1.36	1.29	1.25	5	1.29	0.043

Table 4.9: The storage moduli (E'), loss moduli (E"), T_g, and tan δ of starch/NR foams with and without calcium carbonate.

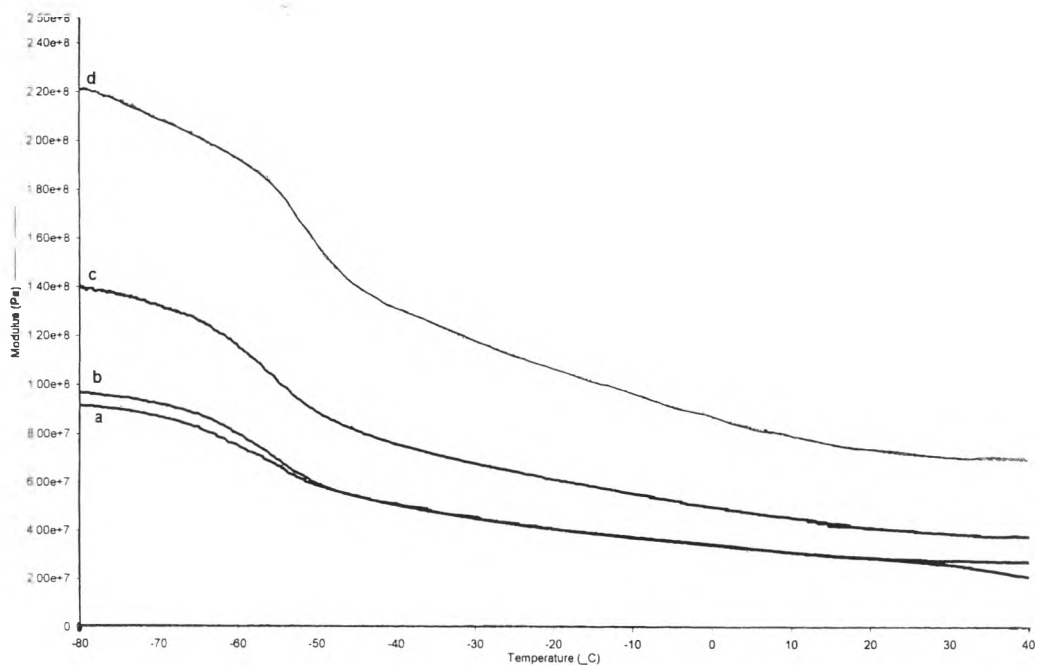| Sample	$E' \times 10^{-8}$ at -80°C (Pa)	$E'' \times 10^{-6}$ at -80°C (Pa)	T_g (°C)		Tan δ	
			Starch	NR	Starch	NR
$CaCO_3$ 0%	0.93	0.89	-	-53.4	-	0.13
$CaCO_3$ 5%	0.98	0.74	-	-53.8	-	0.12
$CaCO_3$ 15%	1.40	0.90	-	-52.9	-	0.13
$CaCO_3$ 30%	2.20	1.33	-	-52.7	-	0.15

Figure 4.20 The storage moduli of the starch/NR foams: (a) 0% CaCO$_3$

(b) 5% CaCO$_3$; (c) 15% CaCO$_3$; (d) 30% CaCO$_3$
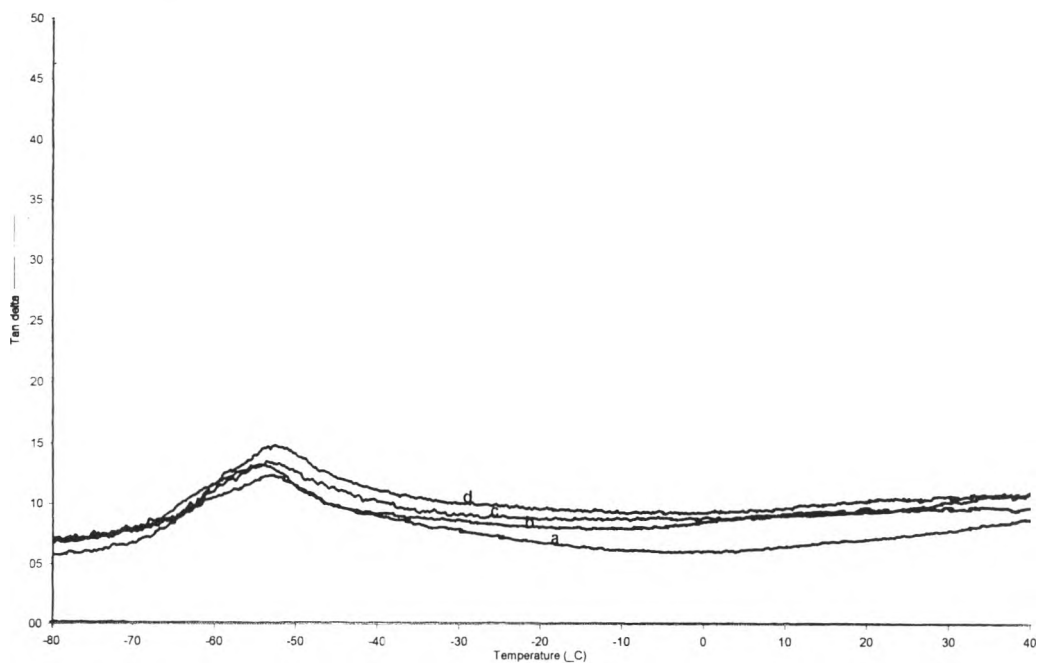

Figure 4.21 Tan δ and T_g of the starch/NR foams: (a) 0% CaCO$_3$

(b) 5% CaCO$_3$; (c) 15% CaCO$_3$; (d) 30% CaCO$_3$

Table 4.10 The percentage increase in compressive strength of the foams with varies

CaCO$_3$ content

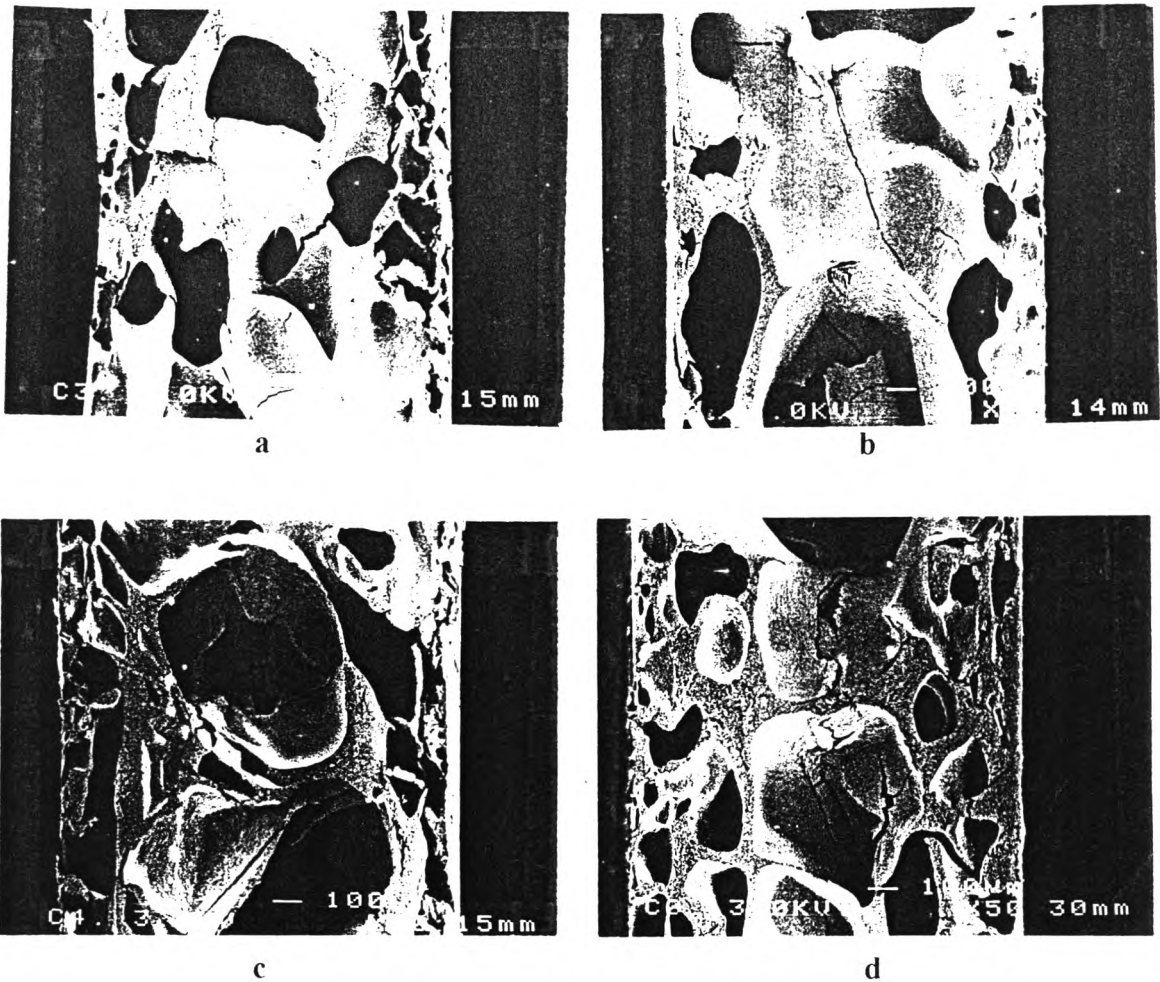| CaCO$_3$ content (%)	Increasing in compressive strength (%) compare with the 0% CaCO$_3$ content
5	3.8
15	69
30	148

Figure 4.22 Scanning electron micrographs of cross sections of starch/NR/CaCO$_3$

foams; (a) 0% CaCO$_3$; (b) 5% CaCO$_3$; (c) 15% CaCO$_3$ (d) 30% CaCO$_3$

at 50x magnification.